Title
Mechanisms of NDV-3 vaccine efficacy in MRSA skin versus invasive infection.

Journal
Proceedings of the National Academy of Sciences of the United States of America, 111(51)

ISSN
0027-8424

Authors
Yeaman, Michael R
Filler, Scott G
Chaili, Siyang
et al.

Publication Date
2014-12-01

DOI
10.1073/pnas.1415610111

Peer reviewed

Mechanisms of NDV-3 vaccine efficacy in MRSA skin versus invasive infection

Michael R. Yeaman[a,b,c,d,1], Scott G. Filler[a,b,d], Siyang Chaili[b,c,d], Kevin Barr[d], Huiyuan Wang[b,c,d], Deborah Kupferwasser[b,c,d], John P. Hennessey Jr.[e], Yue Fu[a,b,d], Clint S. Schmidt[e], John E. Edwards Jr.[a,b,d], Yan Q. Xiong[a,b,d], and Ashraf S. Ibrahim[a,b,d]

[a]Department of Medicine, David Geffen School of Medicine at UCLA, Los Angeles, CA 90095; Divisions of [b]Infectious Diseases and [c]Molecular Medicine, Harbor–UCLA Medical Center, Torrance, CA 90502; [d]St. John's Cardiovascular Research Center, Los Angeles Biomedical Research Institute at Harbor–UCLA Medical Center, Torrance, CA 90502; and [e]NovaDigm Therapeutics, Inc., Grand Forks, ND 58202

Edited* by H. Ronald Kaback, University of California, Los Angeles, CA, and approved November 6, 2014 (received for review August 13, 2014)

Increasing rates of life-threatening infections and decreasing susceptibility to antibiotics urge development of an effective vaccine targeting *Staphylococcus aureus*. This study evaluated the efficacy and immunologic mechanisms of a vaccine containing a recombinant glycoprotein antigen (NDV-3) in mouse skin and skin structure infection (SSSI) due to methicillin-resistant *S. aureus* (MRSA). Compared with adjuvant alone, NDV-3 reduced abscess progression, severity, and MRSA density in skin, as well as hematogenous dissemination to kidney. NDV-3 induced increases in CD3+ T-cell and neutrophil infiltration and IL-17A, IL-22, and host defense peptide expression in local settings of SSSI abscesses. Vaccine induction of IL-22 was necessary for protective mitigation of cutaneous infection. By comparison, protection against hematogenous dissemination required the induction of IL-17A and IL-22 by NDV-3. These findings demonstrate that NDV-3 protective efficacy against MRSA in SSSI involves a robust and complementary response integrating innate and adaptive immune mechanisms. These results support further evaluation of the NDV-3 vaccine to address disease due to *S. aureus* in humans.

vaccine | *Staphylococcus aureus* | skin | Th22 | Th17

The bacterium *Staphylococcus aureus* is the leading cause of skin and skin structure infections (SSSIs), including cellulitis, furunculosis, and folliculitis (1–4), and a common etiologic agent of impetigo (5), erysipelas (6), and superinfection in atopic dermatitis (7). This bacterium is a significant cause of surgical or traumatic wound infections (8, 9), as well as decuibitus and diabetic skin lesions (10). Moreover, SSSI is an important risk factor for systemic infection. The skin is a key portal of entry for hematogenous dissemination, particularly in association with i.v. catheters. *S. aureus* is now the second most common bloodstream isolate in healthcare settings (11), and SSSI is a frequent source of invasive infections such as pneumonia or endocarditis (12, 13). Despite a recent modest decline in rates of methicillin-resistant *S. aureus* (MRSA) infection in some cohorts (13), infections due to *S. aureus* remain a significant problem (14, 15). Even with appropriate therapy, up to one-third of patients diagnosed with *S. aureus* bacteremia succumb—accounting for more attributable annual deaths than HIV, tuberculosis, and viral hepatitis combined (16).

The empiric use of antibiotics in healthcare-associated and community-acquired settings has increased *S. aureus* exposure to these agents, accelerating selection of resistant strains. As a result, resistance to even the most recently developed agents is emerging at an alarming pace (17, 18). The impact of this trend is of special concern in light of high rates of mortality associated with invasive MRSA infection (e.g., 15–40% in bacteremia or endocarditis), even with the most recently developed antistaphylococcal therapeutics (19, 20). Moreover, patients who experience SSSI due to MRSA exhibit high 1-y recurrence rates, often prompting surgical debridement (21) and protracted antibiotic treatment.

Infections due to MRSA are a special concern in immune-vulnerable populations, including hemodialysis (22), neutropenic (23, 24), transplantation (25), and otherwise immunosuppressed patients (26, 27), and in patients with inherited immune dysfunctions (28–31) or cystic fibrosis (32). Patients having deficient interleukin 17 (IL-17) or IL-22 responses (e.g., signal transduction mediators STAT3, DOCK8, or CARD9 deficiencies) exhibit chronic or "cold" abscesses, despite high densities of pathogens such as *S. aureus* (33, 34). For example, patients with Chronic Granulomatous Disease (CGD; deficient Th1 and oxidative burst response) have increased risk of disseminated *S. aureus* infection. In contrast, patients with Job's Syndrome (deficient Th17 response) typically have increased risk to SSSI and lung infections, but less so for systemic *S. aureus* bacteremia (35, 36). This pattern contrasts that observed in neutropenic or CGD patients (37). These themes suggest efficacious host defenses against MRSA skin and invasive infections involve complementary but distinct molecular and cellular immune responses.

From these perspectives, vaccines or immunotherapeutics that prevent or lessen severity of MRSA infections, or that enhance antibiotic efficacy, would be significant advances in patient care and public health. However, to date, there are no licensed prophylactic

Significance

***Staphylococcus aureus* is an opportunistic pathogen of the normal human flora. It is among the most frequent causes of cutaneous abscesses, leading to life-threatening invasive infection. Incomplete understanding of host defenses against *S. aureus* skin or invasive infection has hindered development of effective vaccines to address these issues. NDV-3 is a unique cross-kingdom vaccine targeting *S. aureus* and *Candida albicans*. The present studies offer important new evidence: (*i*) NDV-3 protects against methicillin-resistant *S. aureus* skin and skin structure infection largely through IL-22– and IL-17A–mediated host defense peptide and neutrophil induction, (*ii*) vaccine-mediated IL-22 and IL-17A play distinct roles in protection against cutaneous versus invasive infection, and (*iii*) NDV-3 vaccine efficacy in this model involves a coordinated induction of innate and adaptive immunity.**

Author contributions: M.R.Y., S.G.F., J.P.H., C.S.S., J.E.E., and A.S.I. designed research; M.R.Y., S.C., K.B., H.W., D.K., Y.Q.X., and A.S.I. performed research; M.R.Y., S.G.F., J.P.H., Y.F., C.S.S., J.E.E., and A.S.I. contributed new reagents/analytic tools; M.R.Y., S.G.F., S.C., K.B., H.W., D.K., J.P.H., C.S.S., J.E.E., Y.Q.X., and A.S.I. analyzed data; and M.R.Y., S.G.F., S.C., J.P.H., C.S.S., J.E.E., Y.Q.X., and A.S.I. wrote the paper.

Conflict of interest statement: M.R.Y., S.G.F., J.P.H., Y.F., C.S.S., J.E.E., and A.S.I. are shareholders of NovaDigm Therapeutics, Inc., which is developing new vaccines including NDV-3 targeting *Staphylococcus aureus* and other pathogens.

*This Direct Submission article had a prearranged editor.

Freely available online through the PNAS open access option.

[1]To whom correspondence should be addressed. Email: MRYeaman@ucla.edu.

This article contains supporting information online at www.pnas.org/lookup/suppl/doi:10.1073/pnas.1415610111/-/DCSupplemental.

or therapeutic vaccine immunotherapies for *S. aureus* or MRSA infection. Unfortunately, efforts to develop vaccines targeting *S. aureus* capsular polysaccharide type 5 or 8 conjugates, or the iron-regulated surface determinant B protein, have not been successful thus far (38, 39). Likewise, passive immunization using monoclonal antibodies targeting the *S. aureus* adhesin clumping factor A (ClfA, tefibazumab) (40) or lipoteichoic acid (pagibaximab) (41) have not shown efficacy against invasive infections in human clinical studies to date. Moreover, the striking recurrence rates of SSSI due to MRSA imply that natural exposure does not induce optimal preventive immunity or durable anamnestic response to infection or reinfection. Thus, significant challenges exist in the development of an efficacious vaccine targeting diseases caused by *S. aureus* (42) that are perhaps not optimally addressed by conventional approaches.

The NDV-3 vaccine reflects a new strategy to induce durable immunity targeting *S. aureus*. Its immunogen is engineered from the agglutinin-like sequence 3 (Als3) adhesin/invasin of *Candida albicans*, which we discovered to be a structural homolog of *S. aureus* adhesins (43). NDV-3 is believed to cross-protect against *S. aureus* and *C. albicans* due to sequence (T-cell) and conformational (B-cell) epitopes paralleled in both organisms (44). Our prior data have shown that NDV-3 is efficacious in murine models of hematogenous and mucosal candidiasis (45), as well as *S. aureus* bacteremia (46–48). Recently completed phase I clinical trials demonstrate the safety, tolerability, and immunogenicity of NDV-3 in humans (49).

Results

NDV-3 Is Efficacious in a Murine Model of SSSI Due to MRSA. To test the efficacy of the NDV-3 vaccine, mice were vaccinated and boosted with a range of doses and then infected s.c. with MRSA. Control mice received the alum adjuvant alone. Vaccine efficacy was analyzed by multiple parameters, including dermonecrotic area, abscess volume, luminescence signal and CFU density in situ, and immunologic response. Use of the bioluminescent (*lux*+ operon) MRSA Xen30 strain afforded the opportunity to visualize the progression of abscess development in real time in each animal. Results demonstrated that NDV-3 immunization induces robust immunologic responses that are associated with reduction in MRSA virulence during infection of skin and skin structure and reduced invasive infection of deeper tissues.

Reduction in Dermonecrosis Area and Abscess Volume. NDV-3 immunization significantly restricted abscess volume and dermonecrosis area due to MRSA compared with adjuvant controls (Fig. 1 *A* and *B*, respectively), even with a high inoculum (e.g., 10^7 CFU) s.c. bolus in this model. Efficacy was significant across a range of dose regimens (e.g., 3–300 μg rAls3p-N per dose). At 7 d postchallenge, vaccination with NDV-3 also reduced the abscess volume caused by two other clinical MRSA strains (LAC-USA300 or MW2), regardless of the intrinsic virulence of a given strain (Fig. S1). Collectively, these data indicate that NDV-3 induces protective efficacy against MRSA, including strains of differing genotypic and virulotypic backgrounds.

Attenuation of Abscess Progression. Next, we examined the effects of the NDV-3 vaccine on the progression of abscess development over time. The areas of dermonecrosis and abscess volume in mice receiving adjuvant alone developed rapidly, reached a maximal size at 5–7 d postchallenge, and were not entirely resolved by 14 d (Fig. 1 *C* and *D*). In contrast, the abscesses in mice immunized with either the 100 or 300 μg NDV-3 dose regimens developed more slowly, achieved smaller maximum areas of dermonecrosis and abscess volume, and effectively resolved by 14 d. The 3 μg regimen had a lesser effect on abscess progression than the higher doses. In studies using the MRSA strain Xen30, NDV-3 dose regimens of 100 or 300 μg significantly limited the

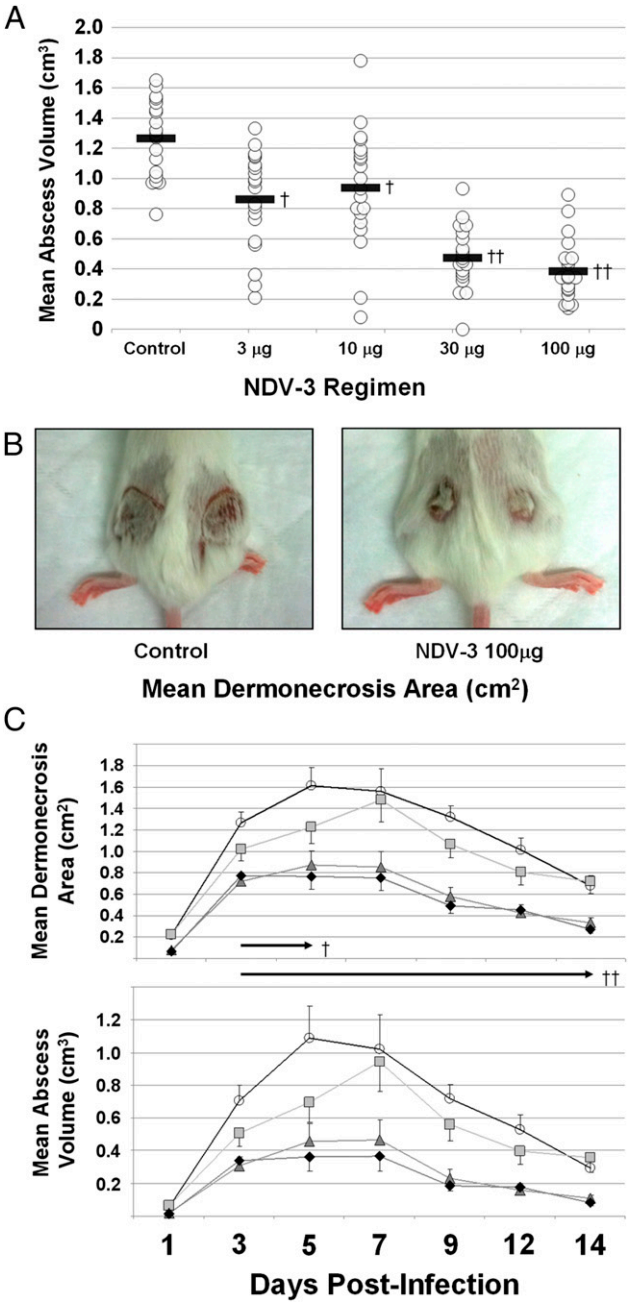

Fig. 1. NDV-3 vaccine-mediated restriction of abscess magnitude and progression due to MRSA Xen30. (*A*) Restriction of abscess volume at day 7 of the infection model. Each circle represents an individual lesion (two lesions per mouse). $^{\dagger}P < 0.05$ or $^{\dagger\dagger}P < 0.01$ versus control mice receiving adjuvant alone. Bars represent means of the respective datasets. (*B*) Restriction of dermonecrosis area and severity at day 7 of the infection model. Visualization of dermonecrosis areas in control and NDV-3–vaccinated mice representing mean results. Note the smaller areas of dermonecrosis and greater degrees of lesion healing in NDV-3–immunized mice, compared with controls, in which lesions remain exudative and poorly contained at this time point. (*C*) Progression of mean dermonecrosis area and mean abscess volume over a 14-d infection model. Dermonecrosis area was significantly attenuated in NDV-3–immunized mice compared with controls at all time points subsequent to day 1. Abscess volume was significantly attenuated in NDV-3–immunized mice compared with controls at all time points subsequent to day 1. Key: ○, control; □, NDV-3 dose regimen 3 μg; Δ, NDV-3 dose regimen 100 μg; ◆, NDV-3 dose regimen 300 μg. For *C*, $^{\dagger}P < 0.05$ for all NDV-3 regimens versus control mice receiving adjuvant alone; $^{\dagger\dagger}P < 0.01$ for NDV-3 regimens Δ or ◆ versus control mice receiving adjuvant alone.

kinetic profile of abscess development across a 14-d study period. Restriction of abscess progression was evident as early as day 2 postchallenge and lasted for the remainder of the study period. Similarly, for MRSA strains LAC-USA300 or MW2, an NDV-3 immunization regimen of 100 μg yielded significant restrictions of abscess progression over a 7-d period (Fig. S2 *A–D*). These data reveal early and ongoing efficacy of NDV-3 immunization that acts to arrest abscess formation by MRSA in this model.

Suppression of MRSA Proliferation. Use of the bioluminescent MRSA Xen30 enabled real-time imaging of the salutary effects of NDV-3 immunization. The 3, 10, 30, and 100 μg NDV-3 dose regimens significantly reduced in situ MRSA bioluminescence (flux; photons·min^{-1}), compared with adjuvant controls (Fig. 2 *A* and *B*). Therefore, NDV-3 immunization suppressed MRSA proliferation within s.c. abscesses in this SSSI model.

Reduction in Abscess MRSA CFU Burden. As an additional evaluation of NDV-3 efficacy, the number of CFUs per abscess was determined in immunized versus adjuvant control mice. At 7 d postchallenge, the number of CFUs in abscesses was significantly reduced in mice immunized with NDV-3 compared with adjuvant controls (Fig. 3). All dosage regimens resulted in approximate 10-fold reductions in skin abscess CFU versus respective controls. In addition, these reductions in abscess CFU density directly corresponded with vaccine-induced reductions in abscess severity and suppression of MRSA bioluminescence (Figs. 1 and 2).

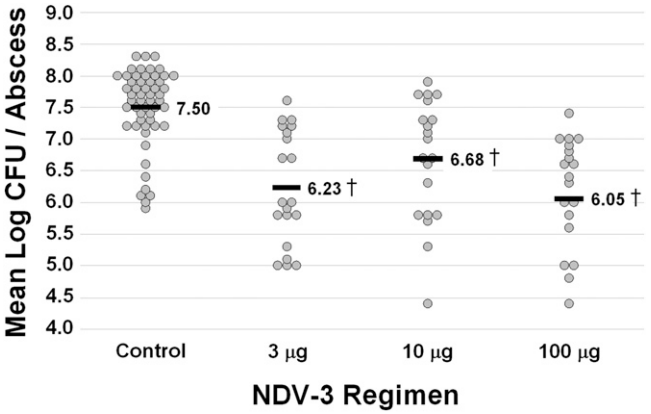

Fig. 3. NDV-3 vaccine-mediated reduction in MRSA Xen30 abscess CFU burden. Distributions of CFU densities of abscesses were determined by quantitative culture at day 7 of the infection model. Substantial reductions in CFU associated with NDV-3 immunization are congruent with the observed restrictions in abscess magnitude (Fig. 1) and suppression of MRSA proliferation (Fig. 2). Each circle represents quantitative culture results from an individual lesion (two lesions per mouse, 10 mice per arm). $^{\dagger}P < 0.05$ versus control mice receiving adjuvant alone. Bars represent means of the respective datasets.

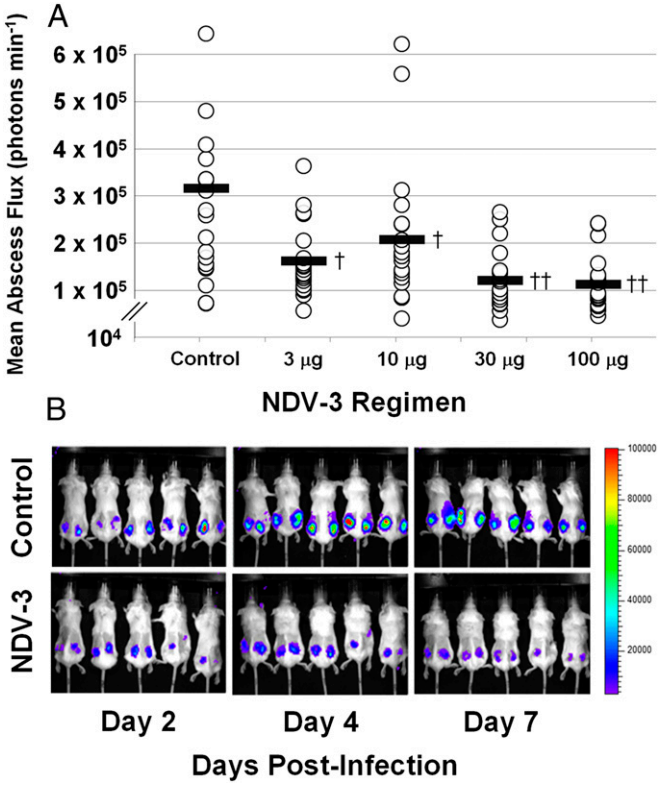

Fig. 2. NDV-3 vaccine-mediated suppression of MRSA Xen30 proliferation in SSSI abscesses in vivo. (*A*) Reduction in luminescent signal at day 7 of the infection model as a function of NDV-3 dose regimen. $^{\dagger}P < 0.05$ or $^{\dagger\dagger}P < 0.01$ versus control mice receiving adjuvant alone. Bars represent means of the respective datasets. (*B*) Visualization of NDV-3–mediated (100 μg dose regimen) suppression of MRSA signal within abscesses in vivo. Imaging was performed and luminescence flux quantified (scale at right) at selected time points over a 7-d infection model. Note the significant reductions in proliferation signal of MRSA strain Xen30 at each time point, as is consistent with restriction of lesion magnitude (Fig. 1) and reduction in abscess CFU burden (Fig. 3) compared with control mice receiving adjuvant alone.

Immune Correlates of NDV-3 Protective Efficacy. Next, we explored the systemic and local immune responses induced by NDV-3 immunization. The immunologic effects of both high- and low-dose NDV-3 regimens were characterized using multiple methods to assess whether different doses induced different patterns of immune response.

Adaptive Immune Response to NDV-3. To determine the effects of NDV-3 immunization on systemic T-cell polarization, mice were immunized and boosted as detailed in *Methods*. Two weeks following the booster dose, their splenocytes were harvested and exposed to the immunizing NDV-3 antigen. The production of IL-17A and IFN-γ by splenocytes was then determined using ELISpot (enzyme-linked immunospot) assays (49). In addition, the sera from these mice were analyzed in parallel for anti–rAls3p-N IgG titers. At high-dose (100 μg) and low-dose (3 μg) regimens, a greater proportion of mice exhibited an IL-17A and IFN-γ T-cell responses compared with adjuvant alone (Table 1). Moreover, the magnitude of IL-17A response for both the low- and high-dose regimens was significantly greater than control. Interestingly, response to the low dose was significantly greater than the high dose (Table S1). The high and low NDV-3 dose regimens both induced a robust anti–rAls3p-N antibody response (Table 1), with the high dose inducing a significantly greater response than the low-dose regimen.

Mechanisms of Protective Immunity. Next, the effects of NDV-3 immunization on immune response to MRSA infection were determined in situ. Mice were immunized and boosted, and SSSI was induced as above. Seven days later, tissues were analyzed by immunohistochemistry and immunofluorescence.

Containment and Clearance of MRSA. Histopathology of abscess tissues in immunized versus control mice substantiated the significant containment and clearance of MRSA in mice that were immunized with NDV-3 (Fig. 4). In control mice, multiple sites of MRSA abscess formation were observed, from the outermost corneal layer of the skin to invasion of deeper basal layers of the hypodermis and beyond into muscle (Fig. 4*A*, images *1–3*). In contrast, mice immunized with NDV-3 had substantially fewer

Table 1. Systemic immune responses to high- or low-dose NDV-3 in the mouse model

Molecule	Control	3 μg	100 μg
IL-17A	10.8 ± 3.2 SFU[a] (3/7)	60.1 ± 3.4 SFU** (8/9)	22.3 ± 2.2 SFU** (5/9)
IFN-γ	6.3 SFU (1/5)	6.6 ± 1.9 SFU (4/7)	14.0 ± 20.3 SFU* (2/7)
IgG	1.5 ± 1.1 GCU[b] (0/10)	41.8 ± 2.5 GCU** (10/10)	83.7 ± 1.8 GCU** (10/10)

[a]Geomean SFUs (SFU/10^6 splenocytes) and SD for responders (*n*/total).
[b]Geomean corrected units (GCUs) and SD for all mice.
*$P < 0.05$ vs. control; **$P < 0.01$ vs. control.

MRSA microabscesses, with organisms confined to the uppermost epidermal layer, and little or no detectable invasion (Fig. 4*A*, images *4–6*). These findings are consistent with the containment and clearance of MRSA due to NDV-3 immunization and correlate with reductions in MRSA abscess magnitude, progression, and CFU density (Figs. 1–3).

Infiltration of Immune Effector Cells into Abscess Sites. Immunohistochemical studies demonstrated that NDV-3 immunization induced a significant increase in the infiltration of $CD3^+$ lymphocytes and Ly6G+ granulocytes in affected tissue (Fig. 4 *B* and *C*). The density of $CD3^+$ cells per high-power field (HPF) was significantly greater in the MRSA abscesses of NDV-3–immunized mice than in the control mice (Fig. 4*B*). This pattern of $CD3^+$ cell response was consistent with higher T-cell density proximal to smaller and fewer MRSA abscesses (Fig. 4*C*, images *4–6*). Likewise, neutrophil infiltration at sites of infection was more robust in NDV-3–immunized mice (Fig. 4*C*, images *4–6*) than in adjuvant controls (Fig. 4*C*, images *1–3*). These results demonstrate that immunization with NDV-3 promotes the rapid and intensive targeting of relevant lymphocytes and granulocytes to areas of MRSA infection.

IL-17A and IL-22 Expression in MRSA Abscesses. NDV-3 induces IL-17A and IL-22 in MRSA abscesses in this SSSI model (Fig. 4 *D* and *E*). For example, IL-17A expression was significantly greater in abscesses of mice immunized with NDV-3 (Fig. 4*D*, images *4–6*) than in control mice (Fig. 4*D*, images *1–3*). Moreover, the IL-17A expression pattern in NDV-3–vaccinated mice was intensified in proximity to MRSA microabscesses (Fig. 4*D*, images *2* and *3* versus images *4* and *5*, respectively). Furthermore, production of IL-17A by $CD3^+$ cells at sites of MRSA infection was greater in NDV-3–immunized mice compared with controls (Fig. S3 *A–D*). Likewise, expression of IL-22 was significantly greater at sites of MRSA microabscesses in mice receiving NDV-3 immunization than in corresponding adjuvant controls (Fig. 4*E*, images *4–6* versus images *1–3*, respectively). Collectively, these results indicate that NDV-3 enhances the local production of IL-17A and IL-22 in SSSI lesions. As a specificity control, NDV-3 did not induce any change in IL-4 expression in skin compared with nonvaccinated animals (Fig. S4).

Induction of Host Defense Peptides in Skin Infection. Cytokines associated with the Th17 pathway (e.g., IL-22) are known to induce cutaneous host defense peptide expression in skin and skin structure. In the present study, NDV-3 immunization resulted in substantially increased expression of cutaneous host defense peptides at sites of SSSI (Fig. 4*F*). Expression of murine β-defensin-3 (mβD-3), a mouse homolog of human β-defensin-2 (50) and surrogate for some mucocutaneous host defense peptides, was increased in NDV-3–immunized mice compared with controls. For example, expression of mβD-3 was greater in distribution and intensity in epidermal and hypodermal compartments of skin compared with MRSA abscesses in NDV-3–immunized mice. Moreover, NDV-3 induced other cutaneous host defense peptides at sites of *S. aureus* skin infection, including dermcidin, psoriasin (S100A7), and to a lesser extent the cathelicidin, cathelin-related antimicrobial peptide (CRAMP; Fig. S5).

NDV-3 Protects Against MRSA Invasion in SSSI. Immunofluorescence and confocal microscopy were used to examine the immune responses to MRSA in NDV-3–immunized and control mice. NDV-3 induced an immune response that targeted $CD3^+$ lymphocyte infiltration, induction of IL-17A, and neutrophil infiltration to the immediate proximity of infection (Fig. 5). This response corresponded to protection against MRSA invasion into hypodermal tissue in vaccinated animals (Fig. 5*A*). In contrast, invasion of MRSA into deeper tissue was observed in control mice (Fig. 5*B*). These composite findings support the hypothesis that NDV-3 evokes innate and adaptive immune mechanisms protective against MRSA barrier disruption and invasive infection.

Roles of IL-17A or IL-22 in NDV-3 Vaccine Efficacy. To evaluate potential roles of IL-17A and IL-22 in vaccine efficacy, antibodies were administered to neutralize IL-17A and/or IL-22 in vaccinated mice.

Skin infection. In vaccinated mice, the administration of anti–IL-17A antibody (α-IL-17A) alone did not significantly reduce vaccine efficacy in the skin compared with nonvaccinated controls (Fig. 6 *A* and *B* and Fig. S6). However, administration of α-IL-22 alone resulted in significantly greater dermonecrosis area and abscess volume (Fig. 6*A* and Fig. S6), *S. aureus* proliferation in skin (Fig. 6*B*), and skin abscess CFU density versus vaccinated controls (Fig. 6*C*). Interestingly, combined neutralization of IL-17A and IL-22 did not affect abscess volumes compared with vaccinated, untreated controls but was associated with greater MRSA proliferation in situ than vaccinated controls at study days 2 and 7 (Fig. 6*B*). Therefore, vaccinated mice treated with α-IL-22 and α-IL-17A did not differ from nonvaccinated controls in terms of skin lesion severity at these time points. These findings correspond to histological observations in skin lesions. For example, at day 7, α-IL-17A treatment alone, or combined with α-IL-22, did not alter CD3+ lymphocyte or neutrophil infiltration into skin abscesses (Fig. S7). However, neutralization of IL-22 caused a reduction in antimicrobial peptide expression and neutrophil infiltration in abscesses at day 7 (Fig. S7).

Invasive infection. Kidney bacterial burden was measured at 7 d postinfection as a surrogate of MRSA invasion or hematogenous dissemination to distant organs. Vaccinated mice exhibited significantly lower MRSA densities in the kidney compared with nonvaccinated controls (Fig. 6*C*). Neutralization of IL-17A alone did not abrogate vaccine efficacy, but there was a trend toward mitigation. Likewise, IL-22 neutralization had no detectable effect on kidney bacterial burden in this model. In contrast, dual inhibition of both IL-17A and IL-22 caused a significant increase in mean kidney bacterial density in vaccinated mice versus control, reflecting a greater propensity for MRSA invasive sequelae. For example, combined α-IL-17A/α-IL-22 treatment caused a mean increase of log 1.1 CFU (2.2 ± 0.4 vs. 1.1 ± 0.5) in kidneys of vaccinated animals compared with untreated controls (Fig. 6*C*; $P \leq 0.05$).

Collectively, the results suggest that the capacity of NDV-3 to limit skin infection requires IL-22 and induction of cutaneous host defense peptides. Furthermore, NDV-3 vaccine protection against hematogenous dissemination requires both IL-17A and IL-22.

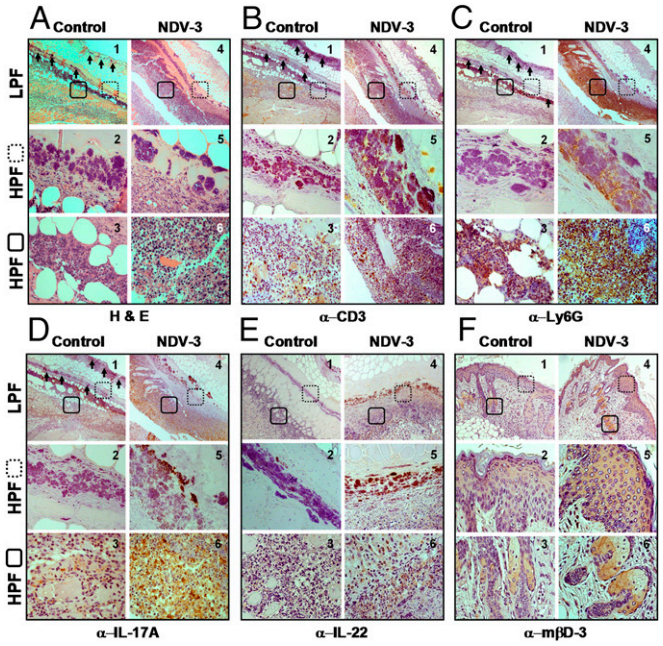

Fig. 4. Histopathology of abscesses due to MRSA Xen30 at day 7 of the infection model. Low-power fields (LPFs) of the epidermal surface (*Top*) are shown in images *1* and *4* of each panel. Relative tissue regions are shown in HPFs (*Insets*) compared with equivalent representative regions in control mice (adjuvant alone; images *2* and *3*) versus NDV-3–immunized mice (images *5* and *6*) of each panel. (*A*) Hematoxylin and eosin (H&E) staining of MRSA abscesses. Arrows indicate the presence of high-density MRSA microabscesses lacking granulocyte intensification in cutaneous tissues of control mice (images *1*–*3*). The number and density of microabscesses are reduced in NDV-3–immunized mice (images *4*–*6*). (*B*) Anti-CD3+ staining (brown) of $CD3^+$ lymphocyte infiltration into abscess lesions. Note the high density of $CD3^+$ cells and germinal centers amid intensive areas of neutrophil infiltration in NDV-3–immunized mice (images *4*–*6*) compared with lesions from control mice (images *1*–*3*). Arrows (image *1*) indicate *S. aureus* microabscesses. (*C*) Anti-Ly6G+ staining (brown) of granulocyte infiltration into abscess lesions. Note the high density of Ly6G+ multilobar nucleated neutrophils engaging microabscess sites in NDV-3–immunized mice (images *5* and *6*). In contrast, MRSA microabscesses relatively free of neutrophil infiltration are observed in epidermal and hypodermal regions in lesions of control nonvaccinated mice (images *2* and *3*). Arrows (plate 1) indicate high-density *S. aureus* microabscesses devoid of neutrophil access. (*D*) Anti–IL-17A staining (brown) in abscess lesions. Note the homogenous, high-level expression of IL-17A expression particularly in mesodermal and hypodermal tissues of NDV-3–immunized mice (images *5* and *6*) compared with a relative paucity of IL-17 expression in lesions of control mice (images *2* and *3*). Induction of IL-17A is consistent with the recruitment of $CD3^+$ T cells (Fig. 4*B*) and Ly6G+ neutrophils (Fig. 4*C*) and reduced MRSA burden correlating with NDV-3 immunization. Arrows (image *1*) indicate *S. aureus* microabscesses. (*E*) Anti–IL-22 staining (brown) of IL-22 expression in abscess lesions. Note the inverse correlation between IL-22 expression and MRSA invasion into the mesodermal and hypodermal regions of NDV-3–immunized mice (images *5* and *6*) compared with low-level IL-22 expression and abundant MRSA microabscesses in lesions of control mice (images *2* and *3*). (*F*) Anti–mβD-3 staining (brown) of mβD-3 expression in abscess lesions. Note the broad intensification of mβD-3 expression in surface epithelium and cutaneous gland structures of NDV-3–immunized mice (images *5* and *6*) compared with baseline-level expression in lesions of control mice (images *2* and *3*). The upregulation of antimicrobial peptides such as mβD-3 supports the concept that NDV-3 immunization stimulates activation of innate and adaptive immune mechanisms to protect against disease due to MRSA.

Discussion

A paucity of mechanistically novel antistaphylococcal agents in the development pipeline, a burgeoning population of individuals at risk for *S. aureus* infections, and the reality of multidrug-resistant strains portends an increasing impact of MRSA infections on global health. Thus, novel vaccines and immunotherapeutic strategies to reduce the incidence and/or mitigate the severity of MRSA infections may yield a significant reduction in morbidity and mortality. Moreover, such approaches would be expected to decrease overall use of antibiotics, in turn reducing pressures that select for drug resistance. However, at the present time, there are no licensed prophylactic or therapeutic vaccines or immunotherapies targeting *S. aureus*.

The immunology of SSSI infection due to MRSA is incompletely understood at the molecular and cellular levels and may differ from that of invasive infection. Despite our previous studies in bacteremia, NDV-3 has not been evaluated in SSSI caused by MRSA, and potential invasive sequelae of SSSI have not been examined in NDV-3 immunization. Thus, the current studies addressed these important goals using multiple techniques in a well-established model of infection that mimics key features of human disease.

Results demonstrate that NDV-3 is protective against MRSA in a mouse model of SSSI. Key findings suggest a coordinated NDV-3–induced immune response in which IL-17A and IL-22 contribute in parallel but nonidentical ways in host defense against SSSI due to MRSA (Fig. 7 and Figs. S8 and S9). The immunologic correlates of efficacy induced by NDV-3 included (*i*) IL-22 activity in defense against cutaneous infection, (*ii*) induction of IL-17A (and to a lesser extent IFN-γ) in protection against invasive infection, (*iii*) recruitment of CD3+ lymphocytes and neutrophils in SSSI lesions, and (*iv*) host defense peptide induction at cutaneous sites of infection. Importantly, NDV-3 efficacy was equivalent against distinct genotypic and virulotypic strains of MRSA. A robust antibody response to NDV-3 also suggests the Th2 pathway is active in host defense against SSSI in this model of infection. This view is supported by studies of Montgomery et al., in which IL-17A and antibody were necessary for protective immunity in recurrent MRSA skin infection in a mouse model (51). However, the roles of humoral immunity in defense against *S. aureus* in animal models or human disease remain to be elucidated (52–55).

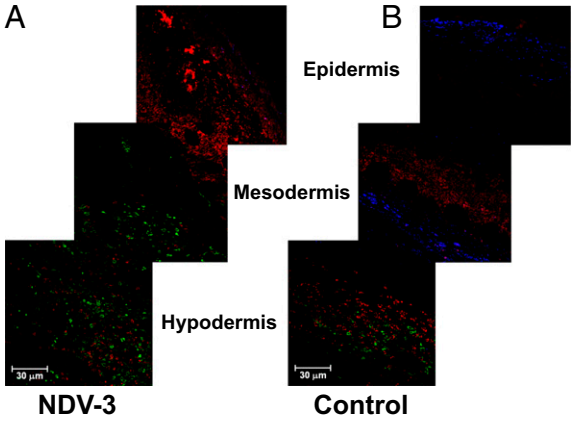

Fig. 5. Coordinated immune response to MRSA challenge induced by NDV-3 at day 7 of the infection model. Immunofluorescence and confocal microscopy were used to generate composite images visualizing complete abscess columns [epidermis (*Top*) to hypodermis (*Bottom*)] in lesions representing NDV-3–immunized (*A*) versus control mice (*B*). NDV-3 immunization (*A*) induces a coordinated and intensive $CD3^+$ T-cell (green) and Ly6G+ neutrophil (red) infiltrative response that extends from the hypodermis into the epidermis and is associated with a paucity of MRSA organisms or microabscesses (blue). In contrast, lesions from control animals (*B*) exhibit low-density T-cell and neutrophil responses that are limited to the hypodermal and mesodermal regions, allowing MRSA invasion into hypodermal tissue and dense MRSA microabscesses to proliferate extensively.

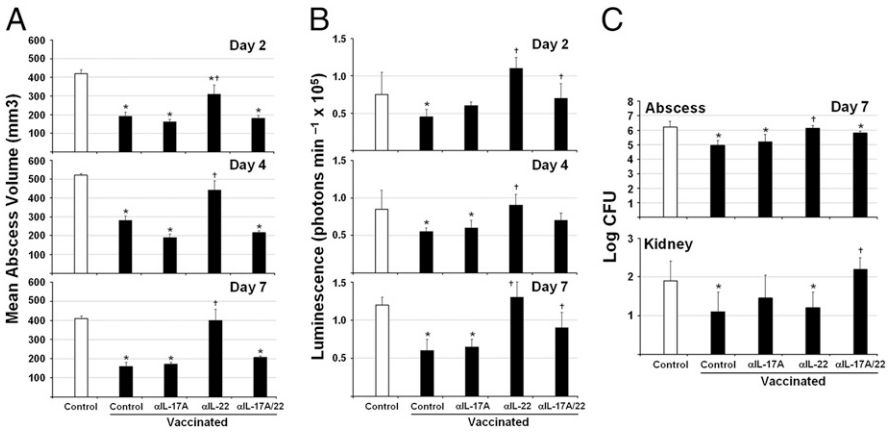

Fig. 6. Impact of IL-17A and/or IL-22 neutralization on parameters of MRSA infection in the setting of NDV-3 vaccination. The kinetics of abscess volume (*A*) and in situ proliferation of MRSA (as measured by luminescence of lux+ strain Xen30) (*B*) are shown over the 7-d study period. The actual CFUs recovered at the study endpoint (day 7) from skin abscesses (*Top*, *C*) and kidneys (*Bottom*, *C*) are also shown. $^{*}P < 0.05$ comparing NDV-3–immunized versus control mice receiving adjuvant alone; $^{\dagger}P < 0.05$ comparing NDV-3–immunized and anti-cytokine–treated mice versus NDV-3–immunized but untreated controls. Bars, SEM.

It is notable that both the 3 μg and 100 μg doses of NDV-3 were efficacious and induced prominent antibody and IL-17A responses relative to control mice but induced only a limited IFN-γ response in either dose group (Table 1). This finding supports the hypothesis that NDV-3 induction of a Th17 response is key to deployment of molecular (e.g., IL-22 and host defense peptide) and cellular (e.g., neutrophil) immune effectors, which afford protection against MRSA. The observation that the lower NDV-3 dose yielded a greater IL-17A response relative to IFN-γ is consistent with counterregulation between IL-17A and IFN-γ (56–58). Overall, the pattern of data suggests the protective effects of NDV-3 in SSSI rely upon an integrated immune response, including Th17 (e.g., IL-17A and IL-22), Th2 (e.g., antibody), and Th1 (e.g., IFN-γ) pathways in mice (Fig. 7 and Figs. S8 and S9). These findings are congruent with data from human vaccination using NDV-3, demonstrating significant antibody, IFN-γ, and IL-17A responses in vaccinated subjects (49). Our current findings are also consistent with—but go beyond—knowledge gained previously from mouse bacteremia models of Als3 immunization against MRSA (45–48).

A relevant theme in the current findings is the consistency of outcomes resulting from different methodologic strategies. For example, CFU density and cytokine levels reconciled with lesion severity in this model. Another insight is that of tissue-specific versus systemic immune responses regarding correlates of protection. The present data reveal distinct roles for IL-22 and IL-17A in skin versus invasive infection. Notably, in humans vaccinated with NDV-3, circulating T-cell responses to primary vaccination peak between 7 and 28 d and then decline (49). However, T-cell responses can be recalled with a second (booster) dose, indicating that long-term memory T cells are generated by NDV-3 vaccination and are responsive to subsequent NDV-3 exposure.

Our results are congruent with recent reports supporting a key function of T cells and the Th17 pathway (including IL-17 family, IL-22, and IL-23 cytokines) in defense against infections at skin and mucocutaneous barriers (59–66). Corticosteroid inhibition of IL-22 production has been associated with impaired barrier protection and increased bacterial invasion (67). Moreover, IL-22 is important to host defense peptide induction by keratinocytes in protection of skin (68). Neutralization of IL-17A and IL-22 resulted in significantly greater MRSA dissemination to kidneys in NDV-3–vaccinated mice. Interestingly, in nonvaccinated mice, Joshi et al. observed that neutralization of IL-17A but not IL-22 increased mortality in *S. aureus* sepsis (69). In NDV-3–vaccinated mice, inhibition of both IL-17A and IL-22 was required to increase MRSA dissemination to the kidney. Even so, compared with nonvaccinated controls, the vaccine retained some efficacy despite IL-17A or IL-22 neutralization. These observations suggest that NDV-3 vaccination induces multiple mechanisms of immune protection. For example, our present data demonstrate that NDV-3 induces a robust antibody response (Table 1) that may contribute to efficacy in this SSSI model. The current data also support prior studies from our group demonstrating that rAls3p-N immunization induces protective efficacy against MRSA

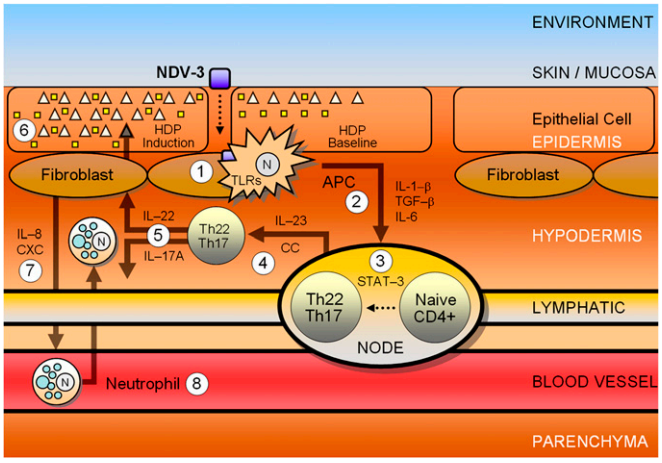

Fig. 7. Integrated model of NDV-3–mediated protective efficacy versus MRSA in murine SSSI. We hypothesize that the NDV-3 immunogen (rAls3p-N) is recognized through toll-like receptors (TLRs) or like sensors for pathogen-associated molecular patterns (PAMPs) on antigen-presenting cells (APCs; *1*). Presentation of processed rAls3 to naïve T cells in the context of a TGF-β1, IL-6, and TNF-α cytokine milieu (*2*) stimulates immune polarization bias to Th22/Th17 via the signal transduction activator of transcription-3 (STAT3; *3*). Supporting the Th17 pathway is the elaboration of CC chemokines and IL-23 that recruit/expand antigen-specific Th17 T cells to sites of infection (*4*). There, immunogen-stimulated Th22 and Th17 cells elaborate IL-17A and IL-22 (*5*), which serve to activate two parallel arms of immune effector function—induction of β-defensins and other cutaneous host defense peptides (*6*) as prompted by IL-22—and CXC chemokine ligand generation (e.g., keratinocyte chemoattractant in mice or its ortholog CXCL8 in humans) from fibroblasts or epithelial cells (*7*), in turn recruiting/activating neutrophils or other leukocytes to foci of infection (*8*). Thus, the current findings support the hypothesis that NDV-3 stimulates an antigen-specific and highly coordinated immune response that is protective against SSSI due to MRSA.

bacteremia (43–48). The adoptive transfer of $CD4^+$ T cells but not $B220^+$ B cells from immunized mice afforded protection (47, 48). Collectively, this body of evidence is consistent with the immunobiology of natural *S. aureus* SSSI in humans (2, 3), Th17 pathway requirements for mucocutaneous host defense against *S. aureus* (33, 34, 61–65), and human responses to the NDV-3 vaccine (49).

The finding that NDV-3 vaccination induced host defense peptides corresponding to cutaneous defense against MRSA is a particularly notable outcome. In humans, host defense peptides including β-defensins 2 and 3 can enhance adaptive immunity (e.g., dendritic cell or lymphocyte function) (70) and potentiate opsonophagocytosis and intracellular killing of pathogens by granulocytes (71). Likewise, complementary or compensatory mechanisms including Th1 responses (41–44), functional antibodies, as well as complement fixation (72) may also contribute to NDV-3 efficacy. Studies to further define the regulation (73–76) of natural and NDV-3–induced cutaneous and invasive host defense against MRSA are ongoing in our laboratory.

Exploring the tissue-targeted and systemic immune responses to NDV-3 in mice challenged s.c. with *S. aureus* revealed new insights into mechanisms of vaccine efficacy. However, the limitations of the current studies should also be recognized. Of interest in this regard are differing perspectives regarding the usefulness of mice as model hosts for evaluation of vaccine immune response or efficacy. On one hand, it is understood that mouse and human immune systems are not identical. Therefore, key differences may be important to interpretation of translatability to humans (53, 55). On the other hand, many life-saving vaccines and immunotherapeutics have been developed based in large part on proof-of-concept data from mouse models. Moreover, analyses of large datasets have recently demonstrated robust similarities between inflammation models in mice and disease in humans (54). In these respects, mouse models of SSSI may be particularly relevant for translational research. For example, the current mouse model recapitulates key aspects of this disease in humans, including affected tissues, lesion evolution, and host defenses. Of special note, the immunologic responses to NDV-3 in the mouse model (e.g., Th17 pathway and anti-rAls3 antibody) are also observed in the human immune responses to NDV-3 (49) (clinicaltrials.gov identifiers NCT01273922 and NCT01447407). Defining contributions of specific cell subsets to NDV-3 efficacy may also be important to devising optimal NDV-3 vaccine or immunotherapeutic strategies targeting *S. aureus*. Further, the roles of B lymphocytes and functional antibodies, and particularly the class switching that is dependent on antigen-restricted T-cell approval (e.g., IgG_1 in humans or IgG_2 in mice), remain to be fully understood with respect to NDV-3 efficacy in SSSI due to *S. aureus*. Nonetheless, the NDV-3 vaccine exploits convergent immunity (44) and thus may have advantages in overcoming limitations experienced in recent clinical trials of *S. aureus* vaccines.

Collectively, the present findings support the concepts of unnatural immunity (77) or convergent immunity (44) as novel means to protect against infections caused by normal flora pathogens. NDV-3 is a recombinant fungal antigen that is expressed in a heterologous host, making it nonidentical to Als3 naturally expressed by *Candida.* This de novo immunogen strategy may also extend cross-protective efficacy of NDV-3 in targeting homologous determinants in the bacterium *S. aureus*. Advances in human skin models (78), including methods to quantify extent of infection and understanding human skin colonization (79), will also be important to development of next-generation vaccines to address *S. aureus* and other opportunistic pathogens that are refractory to conventional anti-infectives. In these respects, the evidence presented in the current study supports continued clinical development and evaluation of NDV-3 in protection against disease caused by *S. aureus* and *Candida*.

Methods

MRSA Strains. MRSA strains Xen30, LAC-USA300, and MW2 were used in these studies. Strain Xen30 (kindly provided by Xenogen/Caliper Life Sciences, Inc.) is derived from the parental strain *S. aureus* MRSA-16 and contains a *luxA-E* operon at a single chromosomal integration site; thus, no exogenous luciferin substrate is required (80). This strain produces the luciferase enzyme and aldehyde substrate and constitutively emits a bioluminescent signal when metabolically active. Its virulence is equivalent to or greater than other MRSA strains in the SSSI murine model as verified by pilot studies. Strain LAC-USA300 is a prototype of the community-acquired MRSA strains of the staphylococcal chromosomal cassette–Mec (*SCCmec*) type USA300 and was first isolated from a correctional facility in Los Angeles County (81, 82). Likewise, MRSA strain MW2 is the prototype of the *SCCmec* type USA400 (83). Study strains have otherwise similar phenotypes and growth characteristics. Logarithmic-phase cells (brain–heart infusion medium; 37 °C) were cultured from virulence-validated research cell banks. Cells were harvested, washed, suspended in PBS, sonicated, and quantified by spectrophotometry to the desired CFU inoculum.

NDV-3 Immunization. NDV-3 was used to immunize mice before infection challenge as we have detailed previously using rAls3p-N (40–43). NDV-3 is composed of the recombinant Als3 antigen (rAls3p-N), which contains the N-terminal portion of the native Als3 protein, formulated with aluminum hydroxide adjuvant in PBS (49). In brief, efficacy of the NDV-3 vaccine was evaluated across a broad rAls3p-N dose range using a constant level of aluminum hydroxide adjuvant. NDV-3 doses (range, 3–300 μg rAls3p-N per dose; intramuscular) were studied in selected experiments, concurrent with respective control mice receiving adjuvant alone. Primary vaccination performed on day 0 was followed by an identical booster vaccination on study day 21. Mice were infected 14 d after boost (study day 35) and monitored for up to 14 d postinfection. A dose regimen of "100 μg" specifically refers to a regimen in which the mice are given a dose of vaccine containing 100 μg rAls3 at both the primary and booster immunization.

Murine Model of SSSI. Animal studies were performed in accordance with approved animal use policies of LABioMed at Harbor–UCLA. Balb/C mice (Harlan) were immunized as described above. An s.c. skin/skin structure abscess model was implemented for these studies as modified from Voyich et al. (84) and Ding et al. (85). In brief, on study day 35, mice were anesthetized, their flanks were shaved and sterilized, and the mice were randomized into appropriate study groups. Next, inocula of 2×10^7 CFU of a given MRSA strain were introduced into s.c. compartments of each flank by injection (100 μL). A minimum of 15 mice per control or NDV-3-regimen groups were used in each study.

Abscess Evaluation. ***Magnitude.*** Abscess area (dermonecrosis) and volume were measured in each mouse flank over the postchallenge study period. To do so, mice were anesthetized, and the lesion site length (l) and width (w) measured to quantify dermonecrosis area (cm^2). Abscess volume (cm^3) was calculated per the formula for a spherical ellipsoid: $[v = (\pi/6) \times l \times w^2]$.

Bioluminescence imaging. At selected time points postinfection, control and immunized mice underwent in vivo bioluminescence imaging [in vivo imaging system (IVIS); Caliper Life Sciences, Inc.]. Bioluminescence signals were captured over a 5-min time period and analyzed using the Living Image software as photons per min per abscess.

Quantitative culture. At preselected time points postinfection, control and immunized mice were humanely censored and processed for quantitative culture of abscesses. Each flank was aseptically dissected and the abscess removed and prepared for culture. Abscesses were individually homogenized and serially diluted in sterile PBS for quantitative culture onto sheep blood agar. In selected experiments, kidneys were excised and processed for quantitative culture to assess hematogenous dissemination. All cultures were incubated (37 °C) for 24 h, and resulting colonies enumerated as CFU per abscess or CFU per kidney.

Immunologic Mechanisms. Complementary approaches were used to assess potential correlates of NDV-3 vaccine efficacy in this murine model of SSSI due to MRSA. These studies focused on strain Xen30, allowing comparison with IVIS data at the time point of greatest lesion burden in control animals, typically 7 d postinfection.

Antibody quantification. Total serum IgG antibody levels were determined in a 96-well ELISA format over a range of dilutions by standard methods. Values represent geometric mean dilution-corrected optical density measurements of triplicate assays of sera from immunized mice.

Cytokine quantification. Production of IFN-γ and IL-17A was determined by ELISpot analysis of splenocytes isolated from immunized mice and exposed to the immunizing Als3 antigen. The number of spot-forming units (SFUs) producing either IFN-γ or IL-17A was quantified per 10^6 cells. Cell viability was verified by production of IFN-γ following stimulation with phorbol-12-myristate-13-acetate and ionomycin per established protocols (45, 49).

Immunohistochemistry. Immunological determinants associated with NDV-3 efficacy were assessed in abscesses from immunized (vaccinated and control) mice by standard methods (86) 7 d after infection. In brief, for immunohistochemical studies, 3-μm-thick vertical paraffin-embedded sections were dewaxed and rehydrated followed by heat-induced antigen retrieval (Dako). Sections were incubated with blocking buffer for 15 min at room temperature to block endogenous peroxidase activity, and nonspecific antibody binding was blocked by incubation with 5% (vol/vol) normal serum corresponding to the primary antibody. Sections were then incubated overnight at 4 °C with a primary antibody targeting a specific molecule or cell of interest (Table S2). Sections were then washed and incubated for 30 min with a respective secondary antibody (Table S2) conjugated with either horseradish peroxidase (HRP) or biotin (Santa Cruz Biotechnology). Colorimetric development was then achieved by 30-min reaction with streptavidin–HRP (Dako) and 3,3′-diaminobenzidine (Vector Laboratories) and counterstained with hematoxylin. Images were visualized using a Zeiss BX43 microscope using a DP21 digital camera.

Immunofluorescence. Immunofluorescence using confocal microscopy was performed using established methods (87) to visualize the integrated immune response to MRSA challenge in NDV-3–immunized versus control mice in the context of SSSI in vivo. In brief, paraffin-embedded sections prepared as above were incubated with immunofluorescence buffer (1% BSA and 2% FCS) for 1 h at room temperature. Primary antibodies directed at target antigens of interest (Table S1) were incubated overnight (4 °C) with tissue sections from control or immunized mice. Sections were then washed and incubated for 60 min with respective secondary antibody (Table S1) diluted in immunofluorescence buffer (2 μg/mL). Subsequently, sections were washed in PBS and mounted using Vectashield H-1500 (Vector Laboratories) to minimize photobleaching. Images were visualized using a Leica SP2 confocal microscope using argon (488 nm), krypton (568 nm), and helium-neon (633 nm) lasers and Confocal version 2.0 software (Leica Instruments).

Inhibition of IL-17A and/or IL-22 Immune Pathways. To further validate mechanisms by which NDV-3 confers immunity to reduce virulence of MRSA, monoclonal antibodies were used to functionally inhibit IL-17A or IL-22 in vaccinated and control models of SSSI. Purified monoclonal anti-mouse IL-17A (eBioscience; 16-7222-85) or anti-mouse IL-22 (eBioscience; 16-7173-85) was prepared as recommended by the manufacturer in endotoxin-free PBS. At study days −2 and +2 relative to infection (day 0), vaccinated and nonvaccinated control mice received 100 μg (i.p.; 100 μL volume) of α–IL-17A, α–IL-22, or both. In addition, vaccinated and nonvaccinated control groups received nonspecific isotype control IgG [100 or 200 μg (IP)], respective to individual or combined treatment groups.

Statistical Analyses. Differences in experimental results were compared by Mann–Whitney *U* analysis. P values < 0.05 are considered statistically significant and where indicated are defined at a higher resolution.

ACKNOWLEDGMENTS. The technical expertise of Dr. Samuel French (Department of Pathology, Harbor–UCLA Medical Center), Dr. Liana Chan (Division of Molecular Medicine, Harbor–UCLA Medical Center), and Teclegiorgis Ghebremariam (Division of Infectious Diseases, Harbor–UCLA Medical Center) is greatly appreciated. The authors recognize Dr. Dennis Dixon and Dr. Rory Duncan for their efforts to facilitate the development of novel anti-infective agents and strategies. This study was supported in part by research grants from the US Department of Defense (Grant W81XWH-10-2-0035), NovaDigm Therapeutics, Inc., and the National Institutes of Health (Grants AI-111661 and AI-063382).

1. Singer AJ, Talan DA (2014) Management of skin abscesses in the era of methicillin-resistant Staphylococcus aureus. *N Engl J Med* 370(11):1039–1047.
2. Miller LS, Cho JS (2011) Immunity against *Staphylococcus aureus* cutaneous infections. *Nat Rev Immunol* 11(8):505–518.
3. Cheng AG, DeDent AC, Schneewind O, Missiakas D (2011) A play in four acts: *Staphylococcus aureus* abscess formation. *Trends Microbiol* 19(5):225–232.
4. David MZ, Daum RS (2010) Community-associated methicillin-resistant *Staphylococcus aureus*: Epidemiology and clinical consequences of an emerging epidemic. *Clin Microbiol Rev* 23(3):616–687.
5. Geria AN, Schwartz RA (2010) Impetigo update: New challenges in the era of methicillin resistance. *Cutis* 85(2):65–70.
6. Gunderson CG, Martinello RA (2012) A systematic review of bacteremias in cellulitis and erysipelas. *J Infect* 64(2):148–155.
7. Sabin BR, Peters N, Peters AT (2012) Chapter 20: Atopic dermatitis. *Allergy Asthma Proc* 33(Suppl 1):S67–S69.
8. Karamatsu ML, Thorp AW, Brown L (2012) Changes in community-associated methicillin-resistant *Staphylococcus aureus* skin and soft tissue infections presenting to the pediatric emergency department: Comparing 2003 to 2008. *Pediatr Emerg Care* 28(2):131–135.
9. Klevens RM, et al.; Active Bacterial Core Surveillance (ABCs) MRSA Investigators (2007) Invasive methicillin-resistant *Staphylococcus aureus* infections in the United States. *JAMA* 298(15):1763–1771.
10. Armstrong DG (2011) An overview of foot infections in diabetes. *Diabetes Technol Ther* 13(9):951–957.
11. Wisplinghoff H, et al. (2004) Nosocomial bloodstream infections in US hospitals: Analysis of 24,179 cases from a prospective nationwide surveillance study. *Clin Infect Dis* 39(3):309–317.
12. Tattevin P, et al. (2012) Concurrent epidemics of skin and soft tissue infection and bloodstream infection due to community-associated methicillin-resistant *Staphylococcus aureus*. *Clin Infect Dis* 55(6):781–788.
13. Landrum ML, et al. (2012) Epidemiology of *Staphylococcus aureus* blood and skin and soft tissue infections in the US military health system, 2005-2010. *JAMA* 308(1):50–59.
14. DeLeo FR, Otto M, Kreiswirth BN, Chambers HF (2010) Community-associated meticillin-resistant *Staphylococcus aureus*. *Lancet* 375(9725):1557–1568.
15. Chambers HF, Deleo FR (2009) Waves of resistance: *Staphylococcus aureus* in the antibiotic era. *Nat Rev Microbiol* 7(9):629–641.
16. van Hal SJ, et al. (2012) Predictors of mortality in *Staphylococcus aureus* bacteremia. *Clin Microbiol Rev* 25(2):362–386.
17. Rivera AM, Boucher HW (2011) Current concepts in antimicrobial therapy against select gram-positive organisms: Methicillin-resistant *Staphylococcus aureus*, penicillin-resistant pneumococci, and vancomycin-resistant enterococci. *Mayo Clin Proc* 86(12):1230–1243.
18. Boucher H, Miller LG, Razonable RR (2010) Serious infections caused by methicillin-resistant *Staphylococcus aureus*. *Clin Infect Dis* 51(Suppl 2):S183–S197.
19. Selton-Suty C, et al.; AEPEI Study Group (2012) Preeminence of *Staphylococcus aureus* in infective endocarditis: A 1-year population-based survey. *Clin Infect Dis* 54(9):1230–1239.
20. Bae IG, et al.; International Collaboration on Endocarditis-Microbiology Investigator (2009) Heterogeneous vancomycin-intermediate susceptibility phenotype in bloodstream methicillin-resistant *Staphylococcus aureus* isolates from an international cohort of patients with infective endocarditis: Prevalence, genotype, and clinical significance. *J Infect Dis* 200(9):1355–1366.
21. Sreeramoju P, et al. (2011) Recurrent skin and soft tissue infections due to methicillin-resistant *Staphylococcus aureus* requiring operative debridement. *Am J Surg* 201(2):216–220.
22. Kang YC, Tai WC, Yu CC, Kang JH, Huang YC (2012) Methicillin-resistant *Staphylococcus aureus* nasal carriage among patients receiving hemodialysis in Taiwan: Prevalence rate, molecular characterization and de-colonization. *BMC Infect Dis* 12(1):284.
23. Lanoix JP, et al. (2011) Bacterial infection profiles in lung cancer patients with febrile neutropenia. *BMC Infect Dis* 11:183.
24. Chen CY, et al. (2010) Epidemiology of bloodstream infections in patients with haematological malignancies with and without neutropenia. *Epidemiol Infect* 138(7):1044–1051.
25. Fishman JA (2011) Infections in immunocompromised hosts and organ transplant recipients: Essentials. *Liver Transpl* 17(Suppl 3):S34–S37.
26. Farr AM, Aden B, Weiss D, Nash D, Marx MA (2012) Trends in hospitalization for community-associated methicillin-resistant *Staphylococcus aureus* in New York City, 1997-2006: Data from New York State's Statewide Planning and Research Cooperative System. *Infect Control Hosp Epidemiol* 33(7):725–731.
27. Shadyab AH, Crum-Cianflone NF (2012) Methicillin-resistant *Staphylococcus aureus* (MRSA) infections among HIV-infected persons in the era of highly active antiretroviral therapy: A review of the literature. *HIV Med* 13(6):319–332.
28. Renner ED, et al. (2008) Novel signal transducer and activator of transcription 3 (STAT3) mutations, reduced T(H)17 cell numbers, and variably defective STAT3 phosphorylation in hyper-IgE syndrome. *J Allergy Clin Immunol* 122(1):181–187.
29. Horváth R, et al. (2011) Expansion of T helper type 17 lymphocytes in patients with chronic granulomatous disease. *Clin Exp Immunol* 166(1):26–33.
30. van den Berg JM, et al. (2009) Chronic granulomatous disease: The European experience. *PLoS ONE* 4(4):e5234.
31. Song E, et al. (2011) Chronic granulomatous disease: A review of the infectious and inflammatory complications. *Clin Mol Allergy* 9(1):10.
32. Chmiel JF, et al. (2014) Antibiotic management of lung infections in cystic fibrosis. I. The microbiome, methicillin-resistant Staphylococcus aureus, gram-negative bacteria, and multiple infections. *Ann Am Thorac Soc* 11(7):1120–1129.
33. Ma CS, et al. (2008) Deficiency of Th17 cells in hyper IgE syndrome due to mutations in STAT3. *J Exp Med* 205(7):1551–1557.
34. Milner JD, et al. (2008) Impaired T(H)17 cell differentiation in subjects with autosomal dominant hyper-IgE syndrome. *Nature* 452(7188):773–776.
35. Freeman AF, Holland SM (2008) The hyper-IgE syndromes. *Immunol Allergy Clin North Am* 28(2):277–291, viii 10.1016/j.iac.2008.01.005.
36. Minegishi Y, et al. (2009) Molecular explanation for the contradiction between systemic Th17 defect and localized bacterial infection in hyper-IgE syndrome. *J Exp Med* 206(6):1291–1301.

37. Winkelstein JA, et al. (2000) Chronic granulomatous disease. Report on a national registry of 368 patients. *Medicine (Baltimore)* 79(3):155–169.
38. Bagnoli F, Bertholet S, Grandi G (2012) Inferring reasons for the failure of *Staphylococcus aureus* vaccines in clinical trials. *Front Cell Infect Microbiol* 2:16.
39. Weisman LE (2007) Antibody for the prevention of neonatal noscocomial staphylococcal infection: A review of the literature. *Arch Pediatr* 14(Supp 1):S31–S34.
40. Weems JJ, Jr, et al. (2006) Phase II, randomized, double-blind, multicenter study comparing the safety and pharmacokinetics of tefibazumab to placebo for treatment of *Staphylococcus aureus* bacteremia. *Antimicrob Agents Chemother* 50(8):2751–2755.
41. Weisman LE, et al. (2011) A randomized study of a monoclonal antibody (pagibaximab) to prevent staphylococcal sepsis. *Pediatrics* 128(2):271–279.
42. Proctor RA (2012) Challenges for a universal *Staphylococcus aureus* vaccine. *Clin Infect Dis* 54(8):1179–1186.
43. Sheppard DC, et al. (2004) Functional and structural diversity in the Als protein family of *Candida albicans*. *J Biol Chem* 279(29):30480–30489.
44. Yeaman MR, et al. (2014) Applying convergent immunity to innovative vaccines targeting *Staphylococcus aureus*. *Front Immunol* 5:463 10.3389/fimmu.2014.00463.
45. Spellberg BJ, et al. (2006) Efficacy of the anti-Candida rAls3p-N or rAls1p-N vaccines against disseminated and mucosal candidiasis. *J Infect Dis* 194(2):256–260.
46. Spellberg B, et al. (2008) The antifungal vaccine derived from the recombinant N terminus of Als3p protects mice against the bacterium *Staphylococcus aureus*. *Infect Immun* 76(10):4574–4580.
47. Lin L, et al. (2009) Immunological surrogate marker of rAls3p-N vaccine-induced protection against *Staphylococcus aureus*. *FEMS Immunol Med Microbiol* 55(3):293–295.
48. Lin L, et al. (2009) Th1-Th17 cells mediate protective adaptive immunity against Staphylococcus aureus and *Candida albicans* infection in mice. *PLoS Pathog* 5(12): e1000703.
49. Schmidt CS, et al. (2012) NDV-3, a recombinant alum-adjuvanted vaccine for Candida and *Staphylococcus aureus*, is safe and immunogenic in healthy adults. *Vaccine* 30(52):7594–7600.
50. Bals R, et al. (1999) Mouse β-defensin 3 is an inducible antimicrobial peptide expressed in the epithelia of multiple organs. *Infect Immun* 67(7):3542–3547.
51. Montgomery CP, et al. (2014) Protective immunity against recurrent *Staphylococcus aureus* skin infection requires antibody and interleukin-17A. *Infect Immun* 82(5): 2125–2134.
52. Fowler VG, Jr, Proctor RA (2014) Where does a *Staphylococcus aureus* vaccine stand? *Clin Microbiol Infect* 20(Suppl 5):66–75.
53. Seok J, et al.; Inflammation and Host Response to Injury, Large Scale Collaborative Research Program (2013) Genomic responses in mouse models poorly mimic human inflammatory diseases. *Proc Natl Acad Sci USA* 110(9):3507–3512.
54. Takao K, Miyakawa T (2014) Genomic responses in mouse models greatly mimic human inflammatory diseases. *Proc Natl Acad Sci USA*, 10.1073/pnas.1401965111.
55. Salgado-Pabón W, Schlievert PM (2014) Models matter: The search for an effective Staphylococcus aureus vaccine. *Nat Rev Microbiol* 12(8):585–591.
56. Murugaiyan G, Mittal A, Weiner HL (2010) Identification of an IL-27/osteopontin axis in dendritic cells and its modulation by IFN-gamma limits IL-17-mediated autoimmune inflammation. *Proc Natl Acad Sci USA* 107(25):11495–11500.
57. Lee J, et al. (2013) Interferon gamma suppresses collagen-induced arthritis by regulation of Th17 through the induction of indoleamine-2,3-doxygenase. *PLoS One* 8(4): 60900.
58. Doodes PD, et al. (2010) IFN-gamma regulates the requirement for IL-17 in proteoglycan-induced arthritis. *J Immunol* 184(3):1552–1559.
59. Conti HR, et al. (2009) Th17 cells and IL-17 receptor signaling are essential for mucosal host defense against oral candidiasis. *J Exp Med* 206(2):299–311.
60. McLoughlin RM, et al. (2006) $CD4^+$ T cells and CXC chemokines modulate the pathogenesis of *Staphylococcus aureus* wound infections. *Proc Natl Acad Sci USA* 103(27): 10408–10413.
61. Cho JS, et al. (2010) IL-17 is essential for host defense against cutaneous *Staphylococcus aureus* infection in mice. *J Clin Invest* 120(5):1762–1773.
62. Sanos SL, Vonarbourg C, Mortha A, Diefenbach A (2011) Control of epithelial cell function by interleukin-22-producing RORγt+ innate lymphoid cells. *Immunology* 132(4):453–465.
63. Mölne L, Corthay A, Holmdahl R, Tarkowski A (2003) Role of gamma/delta T cell receptor-expressing lymphocytes in cutaneous infection caused by *Staphylococcus aureus*. *Clin Exp Immunol* 132(2):209–215.
64. Puel A, et al. (2011) Chronic mucocutaneous candidiasis in humans with inborn errors of interleukin-17 immunity. *Science* 332(6025):65–68.
65. Kupper TS, Fuhlbrigge RC (2004) Immune surveillance in the skin: Mechanisms and clinical consequences. *Nat Rev Immunol* 4(3):211–222.
66. Basu R, et al. (2012) Th22 cells are an important source of IL-22 for host protection against enteropathogenic bacteria. *Immunity* 37(6):1061–1075.
67. Ziesché E, et al. (2009) Dexamethasone suppresses interleukin-22 associated with bacterial infection *in vitro* and *in vivo*. *Clin Exp Immunol* 157(3):370–376.
68. Schröder JM (2010) The role of keratinocytes in defense against infection. *Curr Opin Infect Dis* 23(2):106–110.
69. Joshi A, et al. (2012) Immunization with Staphylococcus aureus iron regulated surface determinant B (IsdB) confers protection via Th17/IL17 pathway in a murine sepsis model. *Hum Vaccin Immunother* 8(3):336–346.
70. Tewary P, et al. (2013) β-defensin 2 and 3 promote the uptake of self or CpG DNA, enhance IFN-α production by human plasmacytoid dendritic cells, and promote inflammation. *J Immunol* 191(2):865–874.
71. Yount NY, Yeaman MR (2012) Emerging themes and therapeutic prospects for anti-infective peptides. *Annu Rev Pharmacol Toxicol* 52:337–360.
72. Ibrahim AS, et al. (2013) NDV-3 protects mice from vulvovaginal candidiasis through T- and B-cell immune response. *Vaccine* 31(47):5549–5556.
73. Minegishi Y, Karasuyama H (2009) Defects in Jak-STAT-mediated cytokine signals cause hyper-IgE syndrome: Lessons from a primary immunodeficiency. *Int Immunol* 21(2):105–112.
74. Yang XP, et al. (2011) Opposing regulation of the locus encoding IL-17 through direct, reciprocal actions of STAT3 and STAT5. *Nat Immunol* 12(3):247–254.
75. Miller LS, et al. (2007) Inflammasome-mediated production of IL-1beta is required for neutrophil recruitment against Staphylococcus aureus in vivo. *J Immunol* 179(10): 6933–6942.
76. Nestle FO, Di Meglio P, Qin JZ, Nickoloff BJ (2009) Skin immune sentinels in health and disease. *Nat Rev Immunol* 9(10):679–691.
77. Nabel GJ, Fauci AS (2010) Induction of unnatural immunity: Prospects for a broadly protective universal influenza vaccine. *Nat Med* 16(12):1389–1391.
78. Popov L, Kovalski J, Grandi G, Bagnoli F, Amieva MR (2014) Three-dimensional human skin models to understand *Staphylococcus aureus* skin colonization and infection. *Front Immunol* 5:41.
79. Brown AF, Leech JM, Rogers TR, McLoughlin RM (2014) *Staphylococcus aureus* colonization: Modulation of host immune response and impact on human vaccine design. *Front Immunol* 4:507.
80. Kadurugamuwa JL, et al. (2003) Direct continuous method for monitoring biofilm infection in a mouse model. *Infect Immun* 71(2):882–890.
81. Anonymous (2003) Outbreaks of community-associated methicillin-resistant Staphylococcus aureus skin infections—Los Angeles County, California, 2002-2003. *MMWR Morb Mortal Wkly Rep* 52(5):88.
82. Diep BA, et al. (2006) Complete genome sequence of USA300, an epidemic clone of community-acquired meticillin-resistant Staphylococcus aureus. *Lancet* 367(9512): 731–739.
83. Baba T, et al. (2002) Genome and virulence determinants of high virulence community-acquired MRSA. *Lancet* 359(9320):1819–1827.
84. Voyich JM, et al. (2006) Is Panton-Valentine leukocidin the major virulence determinant in community-associated methicillin-resistant Staphylococcus aureus disease? *J Infect Dis* 194(12):1761–1770.
85. Ding Y, Onodera Y, Lee JC, Hooper DC (2008) NorB, an efflux pump in Staphylococcus aureus strain MW2, contributes to bacterial fitness in abscesses. *J Bacteriol* 190(21): 7123–7129.
86. Ahrens K, et al. (2011) Mechanical and metabolic injury to the skin barrier leads to increased expression of murine β-defensin-1, -3, and -14. *J Invest Dermatol* 131(2): 443–452.
87. Robertson D, Savage K, Reis-Filho JS, Isacke CM (2008) Multiple immunofluorescence labelling of formalin-fixed paraffin-embedded (FFPE) tissue. *BMC Cell Biol* 9:13.

Supporting Information

Yeaman et al. 10.1073/pnas.1415610111

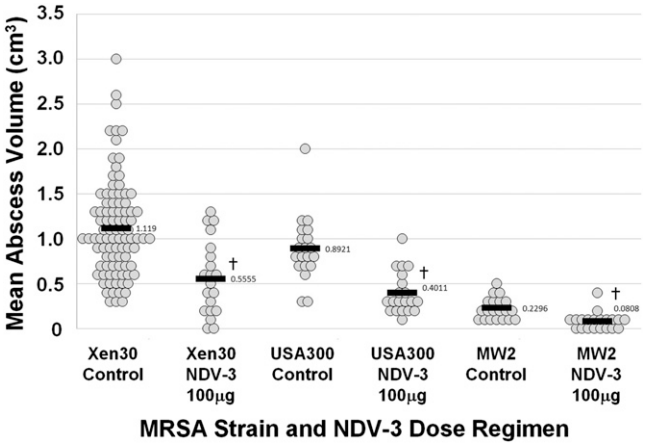

Fig. S1. NDV-3 vaccine-mediated reduction in abscess volume due to multiple MRSA strains at day 7 of the infection model. Note abscess volumes were significantly and equivalently attenuated (e.g., roughly 50% reduction) in NDV-3–immunized mice versus respective controls regardless of which MRSA challenge strain was used to induce infection. Each circle represents an individual lesion. $^{\dagger}P < 0.05$ versus respective control mice receiving adjuvant alone. Bars represent means of the respective datasets.

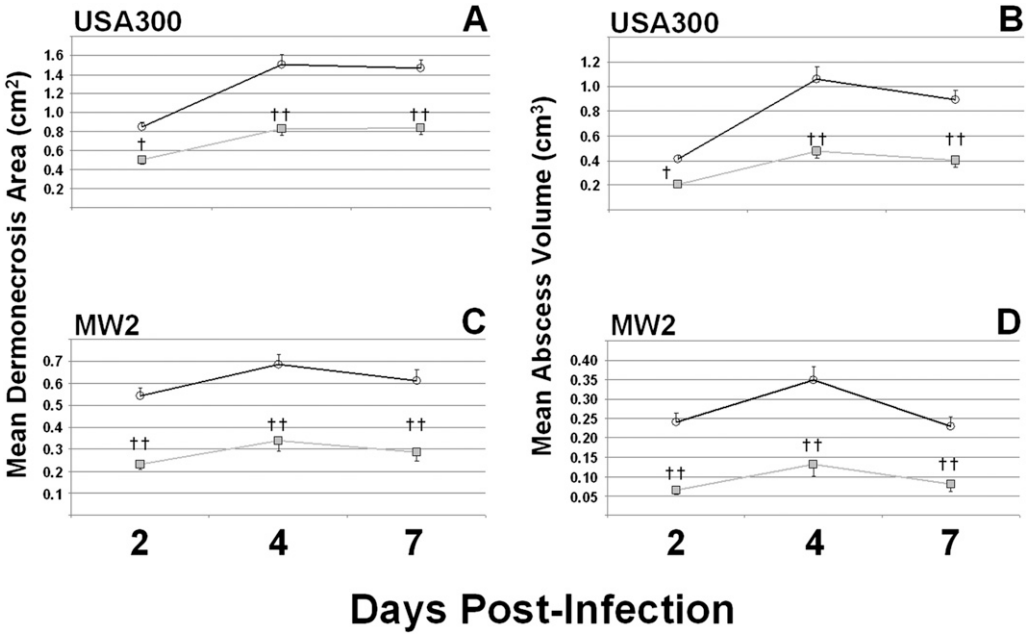

Fig. S2. NDV-3–mediated reduction in abscess magnitude and progression due to MRSA strains LAC-USA300 (*A* and *B*) or MW2 (*C* and *D*) over a 7-d study period of the infection model. Mean areas of dermonecrosis and abscess volume are significantly attenuated in NDV-3–immunized mice compared with respective controls at all time points. $^{\dagger}P < 0.05$ or $^{\dagger\dagger}P < 0.01$ versus control mice receiving adjuvant alone. Key: ○, control; □, NDV-3 dose regimen 100 μg.

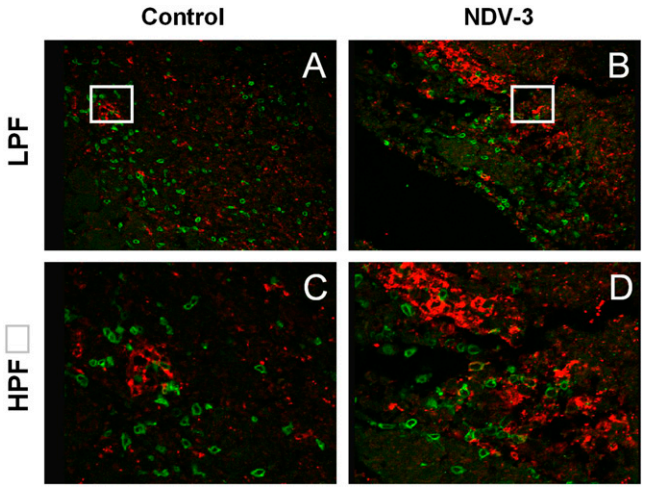

Fig. S3. Enhanced CD3+ cell expression of IL-17A in response to MRSA challenge induced by NDV-3 at day 7 of the infection model. Immunofluorescence and confocal microscopy were used to generate composite images of abscesses (orientation, top is hypodermis) in lesions representing control (*A* and *C*) or NDV-3–immunized mice (*B* and *D*). NDV-3 immunization correlated with increased IL-17A (red) expression in the context of infection (low- and *Inset* high-power fields, LPFs and HPFs; *B* and *D*, respectively), corresponding to a greater density of IL-17A/$CD3^+$ T cells (green) per HPF.

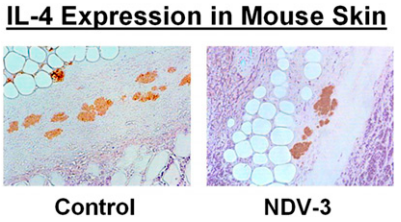

Fig. S4. Specificity of cutaneous cytokine induction by NDV-3. As a control for nonspecific cytokine induction by NDV-3, IL-4 expression was measured in mouse skin. As anticipated, IL-4 expression (surrogate for Th2 pathway; brown) in the local context of skin was unaffected by NDV-3 vaccination, even though antibody was induced systemically. These findings are consistent with the interpretation that the NDV-3 vaccine induces a Th17 response (e.g., IL-17A, IL-22, host defense peptides) that mediates defense of the skin through mechanisms that are not identical to those by which it confers systemic protection against *S. aureus*.

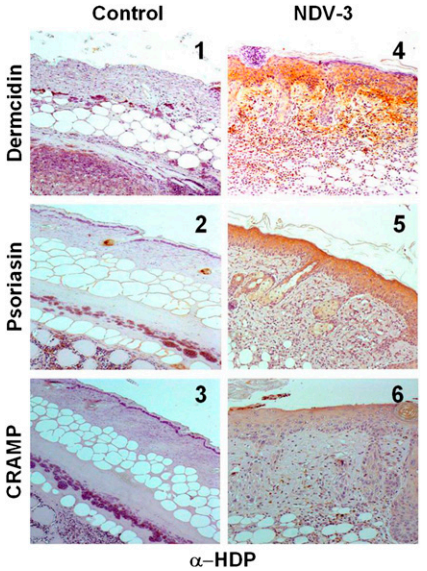

Fig. S5. Expression of host defense peptides (brown) in abscess lesions (LPFs). Note the targeted intensification of dermcidin (image *4*) and psoriasin (image *5*) in NDV-3–vaccinated versus nonvaccinated controls (images *1* and *2*). Induction of the cathelicidin cathelin-related antimicrobial peptide (CRAMP) by NDV-3 vaccination was less than dermcidin or psoriacin (images *3* and *6*) but more than control mice. These findings are consistent with those of mβD-3 (Fig. 4*F*) and support a concept of NDV-3–induced innate immune mechanisms that collectively protect against MRSA infection in skin and skin structure.

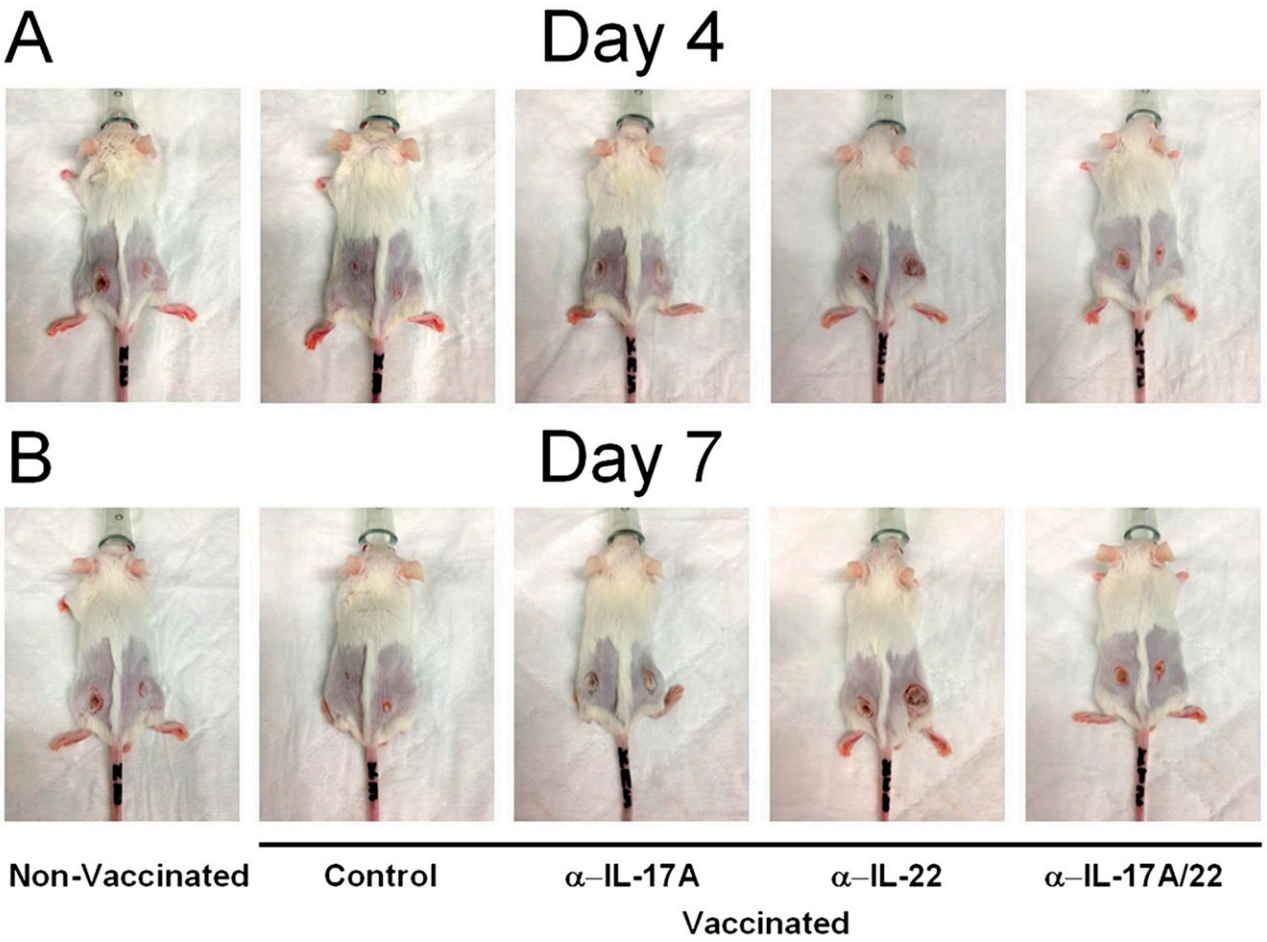

Fig. S6. Visualization of abscess dermonecrotic lesions in skin of NDV-3–vaccinated mice in which cytokines were neutralized versus those in vaccinated but untreated mice and nonvaccinated animals at study days 4 (*A*) and 7 (*B*). Mice selected represent the mean outcomes in a minimum of 10 mice in each comparator group. Note the increase in lesion severity in the vaccinated mice. Efficacy of the vaccine is evident from the decreased lesion severity in vaccinated versus nonvaccinated mice.

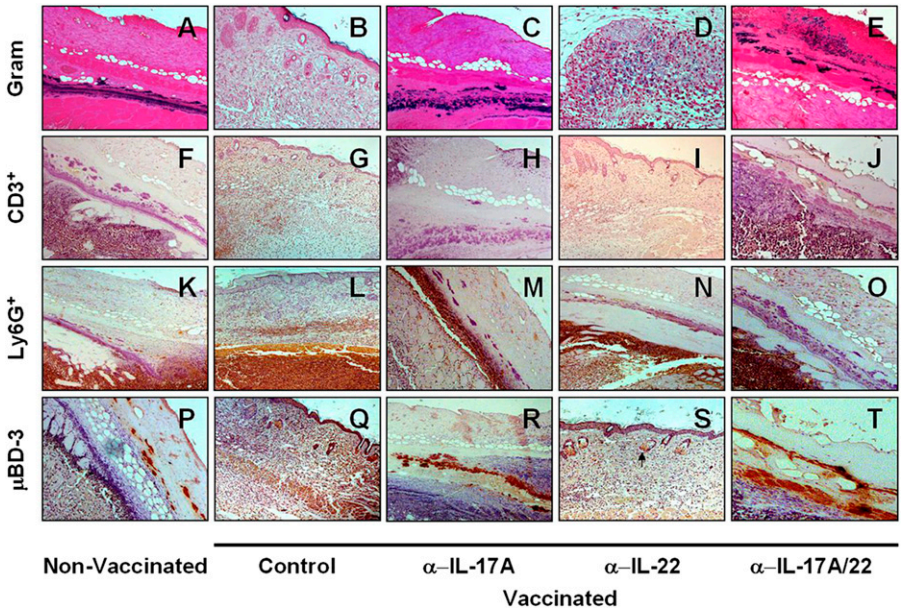

Fig. S7. Comparative atlas of histological and immunohistochemical findings in skin/skin structure. Tissues were processed and stained as detailed in Fig. 4. In brief, skin abscesses from nonvaccinated, vaccinated, and vaccinated/cytokine-neutralized animals were excised and processed on study day 7. (*A*–*E*) Gram stain (MRSA microcolonies, purple; fibrotic tissue that is strongly stained by safranin, pink). (*F*–*J*) CD3+ lymphocytes (brown). (*K*–*O*) Ly6G+ neutrophils (brown). (*P*–*T*) μBD-3 antimicrobial peptide expression (brown).

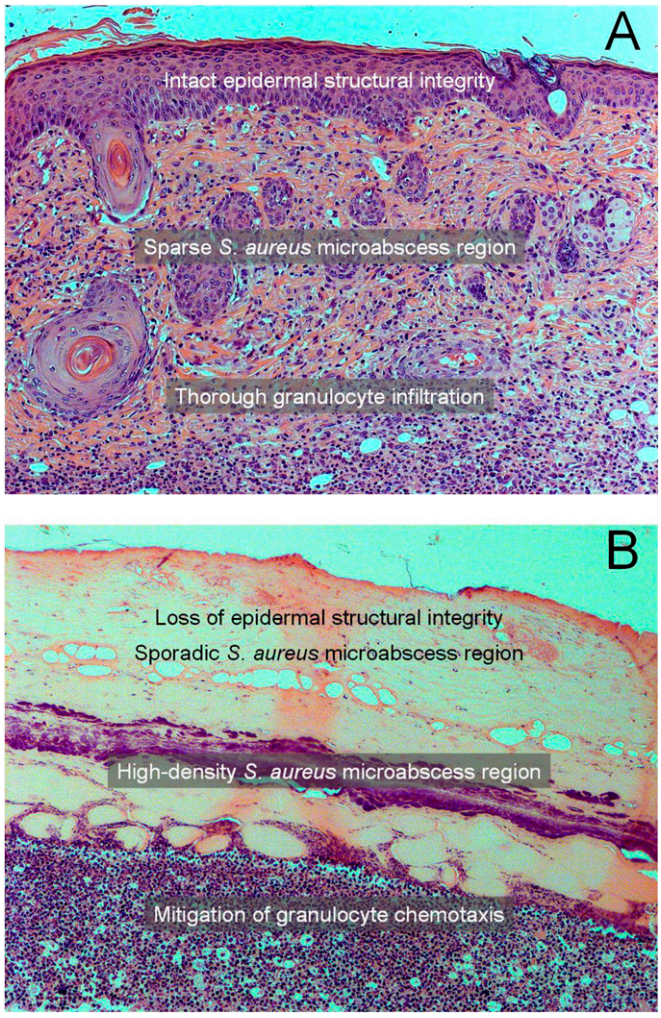

Fig. S8. Histological themes in skin structure of NDV-3–vaccinated mice (*A*) compared with nonvaccinated animals (*B*) at study day 7. Note the generally intact skin/skin structure in the vaccinated animals, replete with thorough granulocyte infiltration and a paucity of MRSA microabscesses (*A*). In contrast, the nonvaccinated mice exhibit large regions of high-density MRSA abscesses in a setting of fibrotic tissue (pink) and a lack of granulocyte chemotactic infiltration into the infected tissue (*B*).

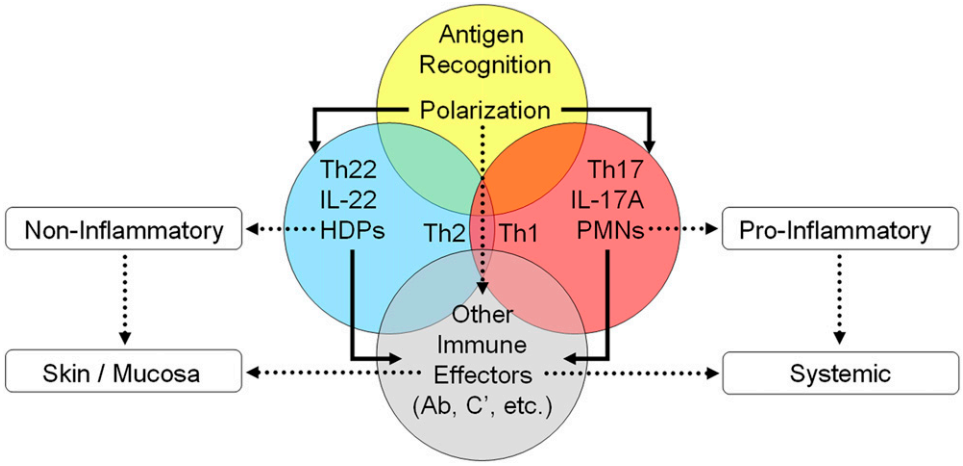

Fig. S9. Hypothesized integrative model of immunopolarization and effector system paradigms in NDV-3–induced host defense against MRSA. This model integrates data from our current and prior reports as well as information from other studies. Note the hypothesized predominance of the Th17 pathway in protection against invasive and hematogenously disseminated infections. By comparison, IL-22 (Th17 pathway or Th22 paradigm) appears to be predominant in protection against MRSA in skin. Ab, antibody; C′, complement; HDPs, host defense peptides; PMNs, neutrophils.

Table S1. Detail of splenocyte responses to NDV-3 dose regimens

Als3 μg per dose	Anti–Als3p-N IgG dilution-corrected optical density	IFN-γ response, SFU/10^6 PBMCs	IL-17A response, SFU/10^6 PBMCs
0	1		
	1	6	7
	1		5
	1		
	1		
	1		
	1		41
	1		
	1		
	1		
3	162		188
	43	4	7
	81	4	
	101		
	19	8	28
	123		35
	43		44
	26		173
	47	14	60
	8		280
100	49		
	126	2	8
	50		23
	152		
	25		
	101		50
	116		
	137		
	109		44
	123	118	15

Note that five of the six NDV-3–vaccinated mice that had Th1 response also had a Th17 response, but only five of the 13 vaccinated mice that had a Th17 response also had a Th1 response. Of the latter group, mice having a Th1 response tended to have lower Th17 responses. This pattern of responses is consistent with Th17 and Th1 counterregulation.

Table S2. Specific antibody reagents used in the present studies

Target	Supplier
Neutralizing antibodies	
α-IL-17A (eBioscience; 16–7222-85)	Affymetrix
α-IL-22 (eBioscience; 16–7173-85)	Affymetrix
Immunohistochemical/immunofluorescence antibodies	
Primary antibodies	
Staphylococcus aureus, mouse	Abcam
S. aureus, rabbit	Fitzgerald Industries International
α-Ly-6G, granulocytes	BD Biosciences
α-CD3	Epitomics
α-IL-17A	Santa Cruz Biotechnology
α-IL-22	Capralogics
α-IL-4	Bioss Inc.
α-mβD-3	Santa Cruz Biotechnology
α-mouse dermcidin	Abcam
α-mouse psoriasin	Bioss Inc.
α-mouse CRAMP	Phoenix Pharmaceuticals
Secondary antibodies	
Alexa 488-conjugated donkey α-rabbit	Molecular Probes
Alexa 488-conjugated donkey α-rat	Molecular Probes
Alexa 555-conjugated goat α-rat	Molecular Probes
Alexa 568-conjugated donkey α-rabbit	Molecular Probes
Alexa 633-conjugated donkey α-goat	Molecular Probes
Alexa 647-conjugated donkey α-rabbit	Molecular Probes
Alexa 633-conjugated streptavidin	Molecular Probes